Computational and Structural Biotechnology Journal 19 (2021) 719–731

COMPUTATIONAL AND STRUCTURAL BIOTECHNOLOGY JOURNAL

journal homepage: www.elsevier.com/locate/csbj

Toxoplasma and *Eimeria* co-opt the host cFos expression for intracellular development in mammalian cells

Bingjian Ren [a], Manuela Schmid [a], Mattea Scheiner [a], Hans-Joachim Mollenkopf [b], Richard Lucius [a], Emanuel Heitlinger [a,c], Nishith Gupta [a,d,*]

[a] Department of Molecular Parasitology, Institute of Biology, Humboldt University, Berlin, Germany
[b] Microarray and Genomics Core Facility, Max-Planck Institute for Infection Biology, Berlin, Germany
[c] Research Group Ecology and Evolution of Parasite Host Interactions, Leibniz Institute for Zoo and Wildlife Research, Berlin, Germany
[d] Department of Biological Sciences, Birla Institute of Technology and Science Pilani (BITS-P), Hyderabad, India

ARTICLE INFO

Article history:
Received 24 September 2020
Received in revised form 30 December 2020
Accepted 31 December 2020
Available online 6 January 2021

Keywords:
Toxoplasma gondii
Eimeria falciformis
Coccidia
Parasite-Host Interaction
Microarrays
Transcriptomics
Gene Expression Analysis

ABSTRACT

Successful asexual reproduction of intracellular pathogens depends on their potential to exploit host resources and subvert antimicrobial defense. In this work, we deployed two prevalent apicomplexan parasites of mammalian cells, namely *Toxoplasma gondii* and *Eimeria falciformis*, to identify potential host determinants of infection. Expression analyses of the young adult mouse colonic (YAMC) epithelial cells upon infection by either parasite showed regulation of several distinct transcripts, indicating that these two pathogens program their intracellular niches in a tailored manner. Conversely, parasitized mouse embryonic fibroblasts (MEFs) displayed a divergent transcriptome compared to corresponding YAMC epithelial cells, suggesting that individual host cells mount a fairly discrete response when encountering a particular pathogen. Among several host transcripts similarly altered by *T. gondii* and *E. falciformis*, we identified cFos, a master transcription factor, that was consistently induced throughout the infection. Indeed, asexual growth of both parasites was strongly impaired in MEF host cells lacking cFos expression. Last but not the least, our differential transcriptomics of the infected MEFs (parental and cFos$^{-/-}$ mutant) and YAMC epithelial cells disclosed a cFos-centered network, underlying signal cascades, as well as a repertoire of nucleotides- and ion-binding proteins, which presumably act in consort to acclimatize the mammalian cell and thereby facilitate the parasite development.

1. Introduction

The protozoan phylum Apicomplexa consists of over 6000 known parasite species, many of which have significant medical, veterinary and ecological relevance because they infect humans, livestock as well as the wildlife [1]. Amongst all, *Toxoplasma gondii* has become a popular model due to relative ease of its propagation, genome engineering and phenotyping [2]. There is only a single species in the genus *Toxoplasma.* Its sexual reproduction is confined to a feline family member (primary or definitive host), whereas asexual growth can occur in most homeothermic organisms (secondary or intermediate host). The asexual stages of *T. gondii* can also transmit between the intermediate hosts and thus bypass the need of a definitive host unlike most other apicomplexans, which has contributed to its widespread success. Besides, the parasite can reproduce in numerous types of nucleated host cells of a given organism. Consequently, there has been substantial interest in decoding how *T. gondii* reprograms and survives in diverse intracellular environments. Some of these studies have deployed transcriptomic profiling of the parasitized mammalian cells to identify and validate the host determinants of parasite development [3–5].

In notable contrast to *Toxoplasma*, another apicomplexan genus *Eimeria* comprises >1800 extant species, which have primarily evolved to reproduce in the gastrointestinal epithelial cells of distinct host organisms [6]. The lifecycle of *Eimeria* species is completed in a single host and the inter-host transmission requires gyrating asexual and sexual reproduction. A high natural diversity of *Eimeria* species in conjunction with its monoxenic lifestyle and fecal-oral transmission make it a prevalent pathogen of livestock and wildlife. One particular species, *E. falciformis*, infecting rodents to accomplish its entire lifecycle, is an emerging model to study the

* Corresponding author at: Philippstrasse 13, House 14, Humboldt University, Berlin, Germany.
E-mail address: Gupta.Nishith@hu-berlin.de (N. Gupta).

https://doi.org/10.1016/j.csbj.2020.12.045

pathogen-host interactions, sexual development, immune response and microbiome-parasite relationship in conventional mouse models [7–10] and in the natural environment [11]. Our own previous research on *E. falciformis* has reported its genome [12] and infection in different rodent species [13,14], investigated the parasite's membrane biogenesis [15] and host immune response [16], as well as studied parasite-induced host manipulation by *ex vivo* expression analyses of the mouse caecum tissue epithelial cells [7,8]. The latter work identified a retinue of IFNγ-regulated pathways including tryptophan catabolism, chemokine signaling and cell-intrinsic immunity, some of which play opposing roles during *in vivo* parasite infection.

Toxoplasma and *Eimeria*, both being tissue-dwelling parasites, belong to the subclass coccidia. Given their differences and similarities, we surmise that *T. gondii* and *E. falciformis* together could enable a more inclusive understanding of the coccidian biology. In this regard, the intestinal epithelial cells – the primary site of infection by both pathogens – impart an outstanding prospect to compare their host reprogramming; however, a parallel (head-to-head) examination in a common host cell type remain elusive. Herein, we utilized the young adult mouse colonic (YAMC) epithelial cells to evaluate how these two phylogenetically-related parasites alter the respective host niche. Among other findings, we discovered the cellular FBJ osteosarcoma oncogene (cFos) – a vital component of the AP-1 transcription factor that governs differentiation, proliferation, apoptosis and immune response in mammalian cells [17,18] – is persistently upregulated upon infection by both parasites. Our subsequent phenotyping and comparative transcriptomics using the cFos-knockout and parental mouse embryonic fibroblasts (MEFs) unveiled a pro-parasite role of cFos alongside its infection-associated network and underlying signaling events.

2. Results

2.1. Eimeria and Toxoplasma infection of YAMC epithelial cells modulate a gamut of host genes

To investigate the gene expression in parasitized YAMC cells, we infected them with tachyzoites of *T. gondii* or with sporozoites of *E. falciformis*, both of which invaded with similar efficiency (40%), as deduced by immunostaining 4 h post-infection (Fig. 1A). Unlike *Toxoplasma* tachyzoites, which divide to form the identical progeny [19], *Eimeria* sporozoites can only develop into trophozoite and schizont stages, and culture is usually aborted 24 h post-infection. We chose 4 h and 16 h for our transcriptomic analysis to discern the infection-linked rewiring of gene expression in host cells. As illustrated in Fig. 1B, RNA was isolated from infected and uninfected YAMC cells, and subsequently the mRNA samples were labeled with Cy3 and Cy5 dyes for hybridization to the whole-genome (4x44K) mouse microarray chips. Differences in gene expression of the parasitized cells with a cut-off of 1.5-fold and an error-weighted p-value ≤ 0.05 in comparison to uninfected samples were considered significant for further analysis.

A majority of genes did not change in expression irrespective of the parasite infection or time point (black dots, Fig. 1C); although, distinct modulation of YAMC cells by *T. gondii* and *E. falciformis* was quite obvious (colored dots, Fig. 1C). We observed 3853 genes regulated in *Eimeria*-infected cells, of which 2002 transcripts were altered after 4 h, 1851 at 16 h, and 155 at both time periods (Fig. 1D). Equally, *T. gondii* infection modulated 3464 transcripts; most of them (2920) however were affected 16 h post-infection, a much smaller set of 544 genes responded within 4 h, and 226 transcripts were perturbed at both time points. These results indicated that the host response during *Eimeria* infection remained rather stable, while a striking difference was recorded between 4 h and 16 h infection by *T. gondii*. Surprisingly, only 10 exclusive transcripts (5 induced, 5 repressed) were regulated by the two parasites 4 h post-infection, whereas 182 unique genes were commonly upregulated, and 158 were downregulated after 16 h incubation. A major fraction of the host transcriptome was affected by one or the other pathogen, signifying a markedly divergent modulation of YAMC epithelial cells in a parasite-specific manner.

2.2. Several distinct and shared host-signaling cascades are regulated by coccidian parasites

Our downstream analysis using KEGG pathway database revealed a significant enrichment of about 90 pathways among all transcripts differentially expressed upon *E. falciformis* and *T. gondii* infection. Nearly one third of these pathways are related to signaling events and a quarter each to oncogenesis and infection processes (Table S1). PI3K-Akt and RIG-I-like receptor pathways were most enriched during *T. gondii* infection, whilst cGMP-PKG, Rap1, oxytocin, NOD-like receptor and NF-κB signaling were modulated mainly by *E. falciformis* (Fig S1A, Table S1). Illustration of two such cascades (PI3K-Akt and cGMP-PKG) showed transcript regulation of several actuators and mediators after 4 h and/or 16 h infection. Interestingly, growth factors (PDGF family) and extracellular matrix collagen (Col15a1) that are known to activate PI3K-Akt signaling as well as various mediators (PI3Ks, Pten, Nur77) were induced by both parasites (Fig S1B). Most effectors involved in protein synthesis and/or cell cycle (4EBPs, eIF4B, p27, cyclin, p27Kip1) were however affected only by *Toxoplasma*. In contrast, *Eimeria* exerted a nearly exclusive induction of PKG and other players of cGMP signaling (RhoA, MLC, CaM) (Fig S1C).

Of multiple commonly-affected host pathways (Fig. 2A), we illustrated cAMP signaling as it converges with other differentially-altered pathways, such as PI3K-Akt, Ca^{2+}, cGMP-PKG, insulin and cFos (*see below*). Notably, *T. gondii* and *E. falciformis* appear to impact different mediators of cAMP signaling (Fig. 2B). Soon after *Eimeria* infection (4h), the adenylate cyclase (AC) transcript was induced, whereas cAMP-specific phosphodiesterase PDE4a was repressed, which suggested the actuation of cAMP signaling. We did not witness this phenomenon upon *T. gondii* infection, albeit genes located upstream of AC (Ptger3, GHRL) and downstream of PKA (Creb5, Creb3l3, Gli3, Crebbp) were significantly altered. Several ion transporters (Ca^{2+}, Na^{+}, K^{+}, Cl^{-}) and calcium-responsive calmodulin (CaM) were affected by both coccidians, implying a perturbed ion homeostasis and calcium signaling in infected host cells. One of the most distinguished transcripts among all was cFos – a master transcription factor known to be induced by cAMP signaling [20] – that was upregulated by the two parasites at 4 h as well as 16 h post-infection. Given the multifaceted roles of cFos in mammalian cells, our latter work investigated its physiological importance and interaction network during parasitic infection.

2.3. cFos is one of the few host transcripts mutually regulated by coccidian parasites

Our further work focused on those transcripts that were inversely or similarly changed in YAMC cells by *Toxoplasma* and *Eimeria* (Fig. 3). Of >3000 altered genes, 74 were perturbed in an opposing manner by specified pathogens (Fig. 3A-B), representing the divergent portion of host response. In early cultures (4 h infection), *E. falciformis* displayed a mostly repressive effect (10 repressed and 4 induced), whereas *T. gondii* exerted an inductive effect (10 induced and 4 repressed). Surprisingly, this trend was reversed at 16 h, as 52 transcripts were upregulated and 8 genes were downregulated by *Eimeria*, and the converse was true for *Toxoplasma*.

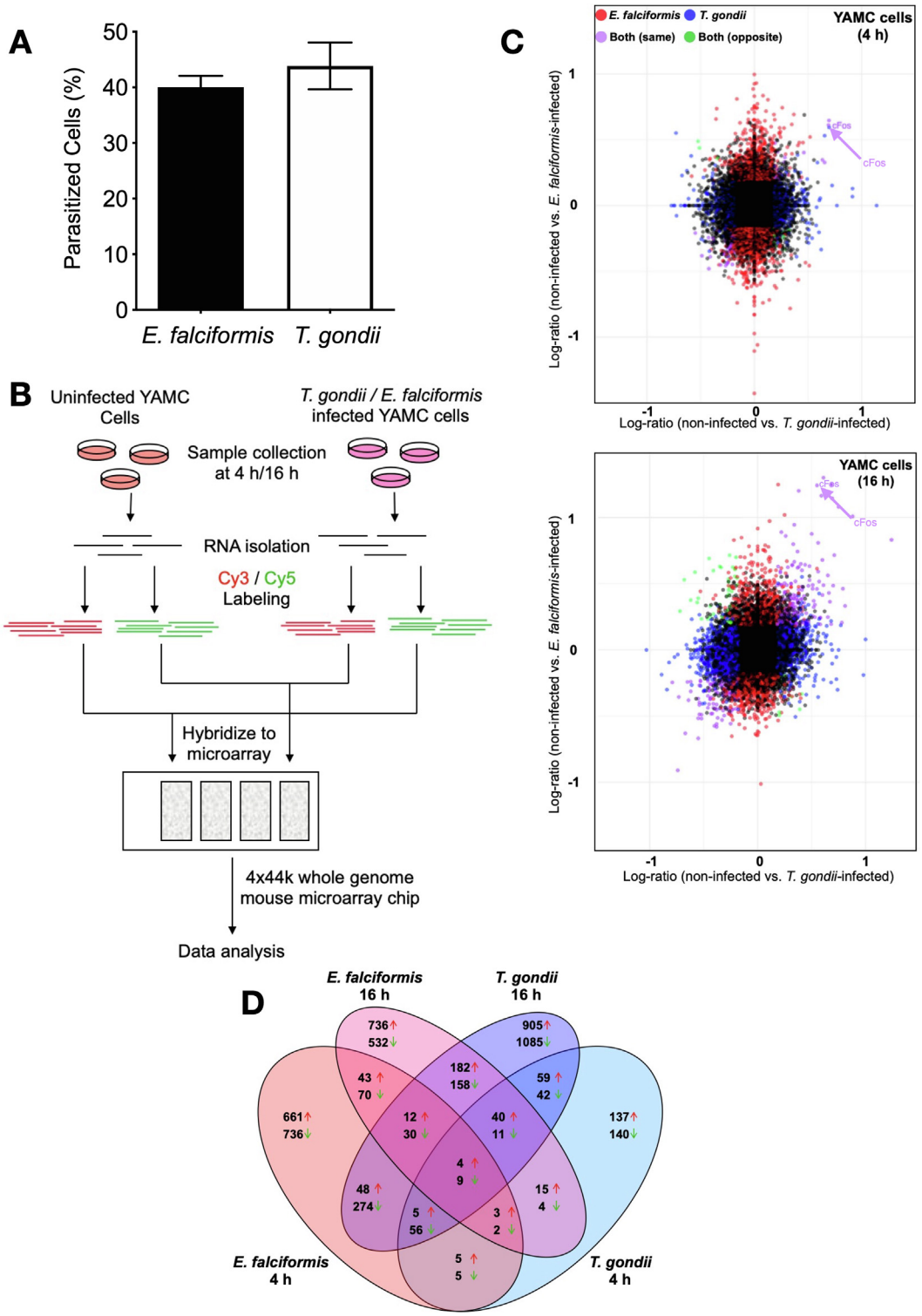

Fig. 1. The young adult mouse colonic epithelial cells show a significant transcriptional modulation upon infection by coccidian parasites. (A) Invasion efficiency of *Eimeria* sporozoites and *Toxoplasma* tachyzoites in YAMC cells. Intracellular parasites (4 h infection) were quantified after staining with anti-*E. tenella* serum (*E. falciformis*), or using anti-*Tg*Sag1 and anti-*Tg*Gap45 antibodies (*T. gondii*). (B) Schematics of the mouse microarray analysis using YAMC host cells parasitized with either *E. falciformis* sporozoites or *T. gondii* tachyzoites. The RNA samples collected after 4 h and 16 h of infection were labelled with Cy3 or Cy5 fluorescent dye, and then hybridized to the whole-genome microarrays. (C) Scatter plot of the fold-changes between uninfected and infected YAMC cells after 4 h or 16 h infection either with *T. gondii* or with *E. falciformis*. Differentially-regulated probes (fold change $\geq +1.5$, $p \leq 0.05$) are color-coded, whereas others appear in black. Probes altered only by *T. gondii* or *E. falciformis* are colored blue and red respectively, while those regulated by both are depicted in violet (same trend) or green (opposite trend). (D) Venn diagram of genes regulated upon infection by *T. gondii* or *E. falciformis*. (For interpretation of the references to color in this figure legend, the reader is referred to the web version of this article.)

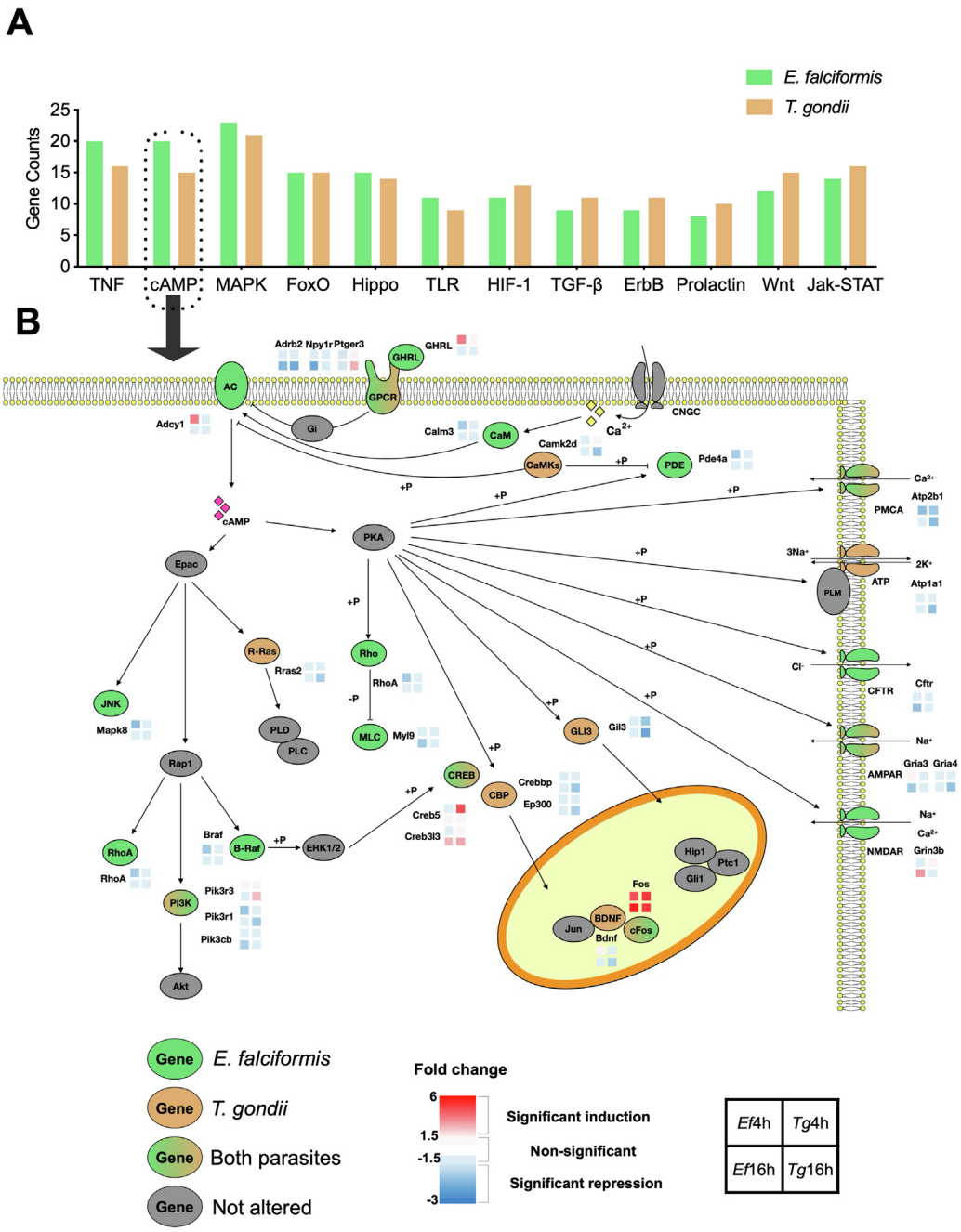

Fig. 2. cAMP signaling is one of several differentially-modulated signaling cascades in coccidian-infected YAMC cells. (A) Signaling pathways regulated upon infection by *T. gondii* or *E. falciformis*. Significantly-altered genes were analyzed for KEGG pathway enrichment and selected transduction cascades shared by both parasites were plotted. For an inclusive list of enriched pathways, refer to Table S1. The pathways were enriched using DAVID v6.7 (EASE score $\leq$ 0.1). (B) Scheme depicting transcriptional reprogramming of cAMP signaling in parasitized host cells. Genes shown with colored symbols are regulated by either or both pathogens. Heatmap blocks next to individual genes illustrate the fold-change according to the actual up- or down-regulation relative to uninfected controls.

Quite notably, many interferon-associated genes were repressed in YAMC cells inhabited by *T. gondii*, but induced upon *E. falciformis* infection (Fig. 3B). Equally, many other genes involved in epithelial cell growth and inflammatory response (*e.g.*, Muc13, Prkce, Trp53inp1, Pxt1, Dusp1, Dusp10) were downregulated by *Toxoplasma*, although induced during *Eimeria* infection.

We identified 13 transcripts that were similarly regulated during both infections (Fig. 3C). Among these, Rassf3, a member of the RASSF family tumor suppressors that is known to induce apoptosis [21], was repressed, indicating inhibition of apoptosis in parasitized cells. Besides, repression of Adrb2, which controls inflammation by rapid induction of IL10 [22], may shift the immune equilibrium in favor of the host cells. Likewise, downregulation of Ikzf2 – a chromatin remodeler maintaining self-renewal in leukemic stem cells [23] – may promote the cellular differentiation upon infection. On the other hand, transcripts of Saa4, Slc8a3, Me3 and cFos were steadily upregulated. Serum amyloid A (SAA) is a family of microbe-inducible retinol-binding proteins expressed in the intestinal epithelium [24]. Retinol is pivotal to develop the innate and adaptive immunity; hence the induction of Saa4 is

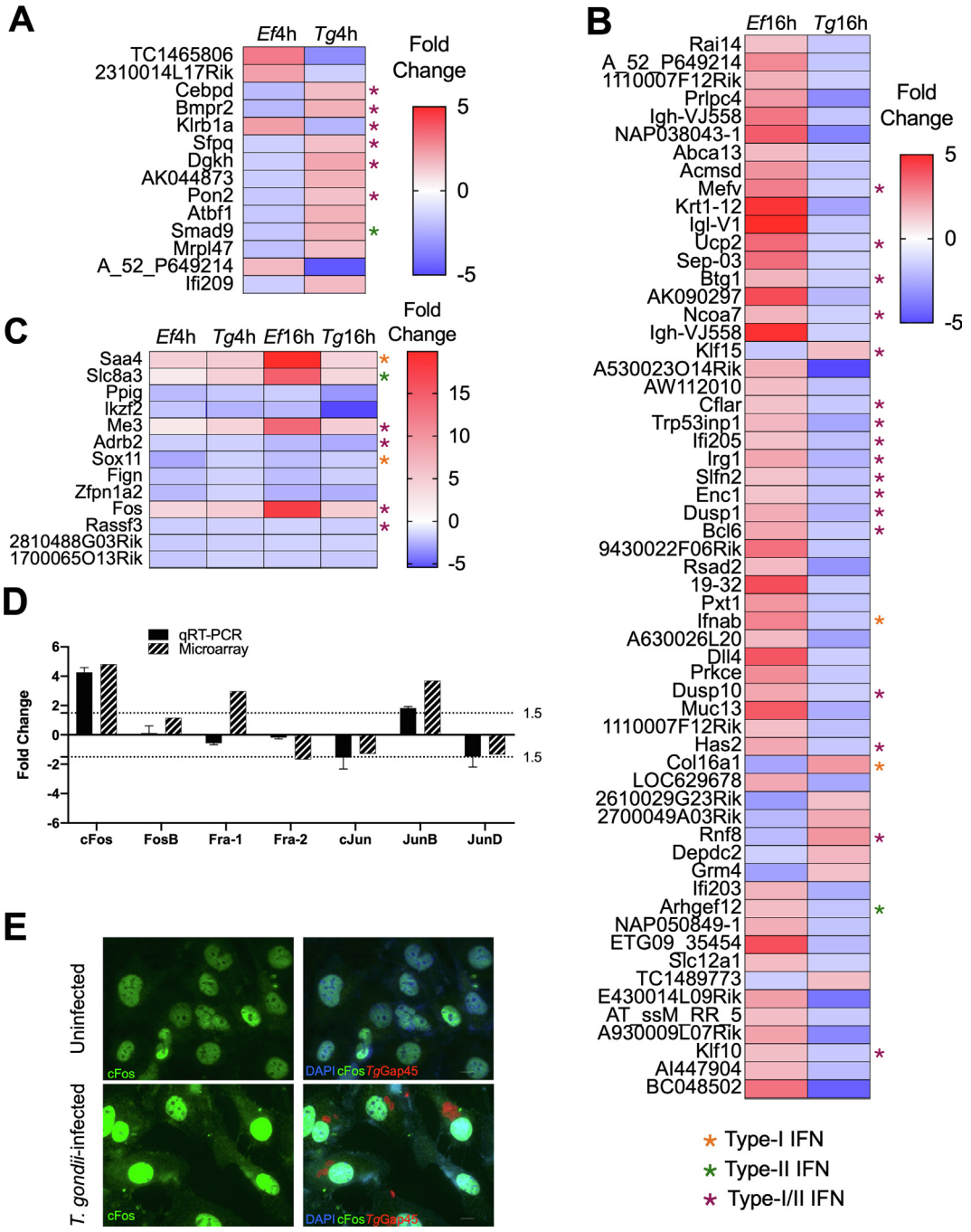

Fig. 3. Only a limited set of host transcripts are conjointly regulated by *Toxoplasma* and *Eimeria*. (A-B) Genes altered in an opposite manner (inversely-regulated) upon parasitism of YAMC epithelial cells with *T. gondii* or *E. falciformis* (4 h, 16 h infection). *Asterisks* indicate those genes that can be modulated by type-I or type-II interferon (Orange, type-I; green, type-II; violet, type-I and type-II) (C) Genes similarly affected by both parasites. Heatmaps in *panel A-C* show fold-induction or repression according to the color scale. (D) Quantitative PCR expression profile of the *Fos/Jun* family members in comparison to the microarray dataset. The qPCR results were obtained by the $^{\Delta\Delta}Ct$ method, and threshold modulation of transcripts ($\geq$1.5 or $\leq$ 1.5) is marked by dotted lines. (E) Immunostaining of cFos upon infection of YAMC epithelial cells by *T. gondii* tachyzoites. Host cells (uninfected or 16 h post-infection) were stained with mouse anti-cFos monoclonal (green) and rabbit anti-*Tg*Gap45 (red) antibodies. DAPI was used to visualize the parasite and host nuclei. Images shown herein represent one of the three independent assays. (For interpretation of the references to color in this figure legend, the reader is referred to the web version of this article.)

likely a defensive response of the YAMC epithelial cells. Upregulation of solute carrier 8a3 (Slc8a3) and malic enzyme 3 (Me3) by contrast may foster the parasite growth by adjusting ionic and pyruvate homeostasis, respectively.

A persistent induction of cFos echoed with potential activation of cAMP signaling (Fig. 2), implying a role of this key transcription factor during coccidian infection. We therefore tested the expression of cFos family genes (cFos, FosB, Fra-1, Fra-2, cJun, JunB, JunD) by performing a quantitative PCR analysis of *T. gondii*-infected YAMC cells (Fig. 3D). Overall, the qPCR data correlated well with our microarray results. We observed that both cFos and JunB were significantly induced, while cJun and JunD were modestly suppressed upon infection. Expression of Fra-1, Fra-2 and FosB was either unaffected or did not match between the qPCR and microarray datasets. Our extended work attempted to validate the induced expression of cFos by immunoblot analysis, which did not however

yield a reproducible detection of the protein. Nonetheless, immunofluorescent staining of tachyzoite-infected YAMC epithelial cells (Fig. 3E) indicated apparent upregulation of cFos when compared to the uninfected sample, and prompted us to examine its physiological relevance as described below.

2.4. cFos is required for optimal in vitro growth of Eimeria and Toxoplasma

We next studied the importance of cFos for the parasite development in murine embryonic fibroblasts lacking its expression

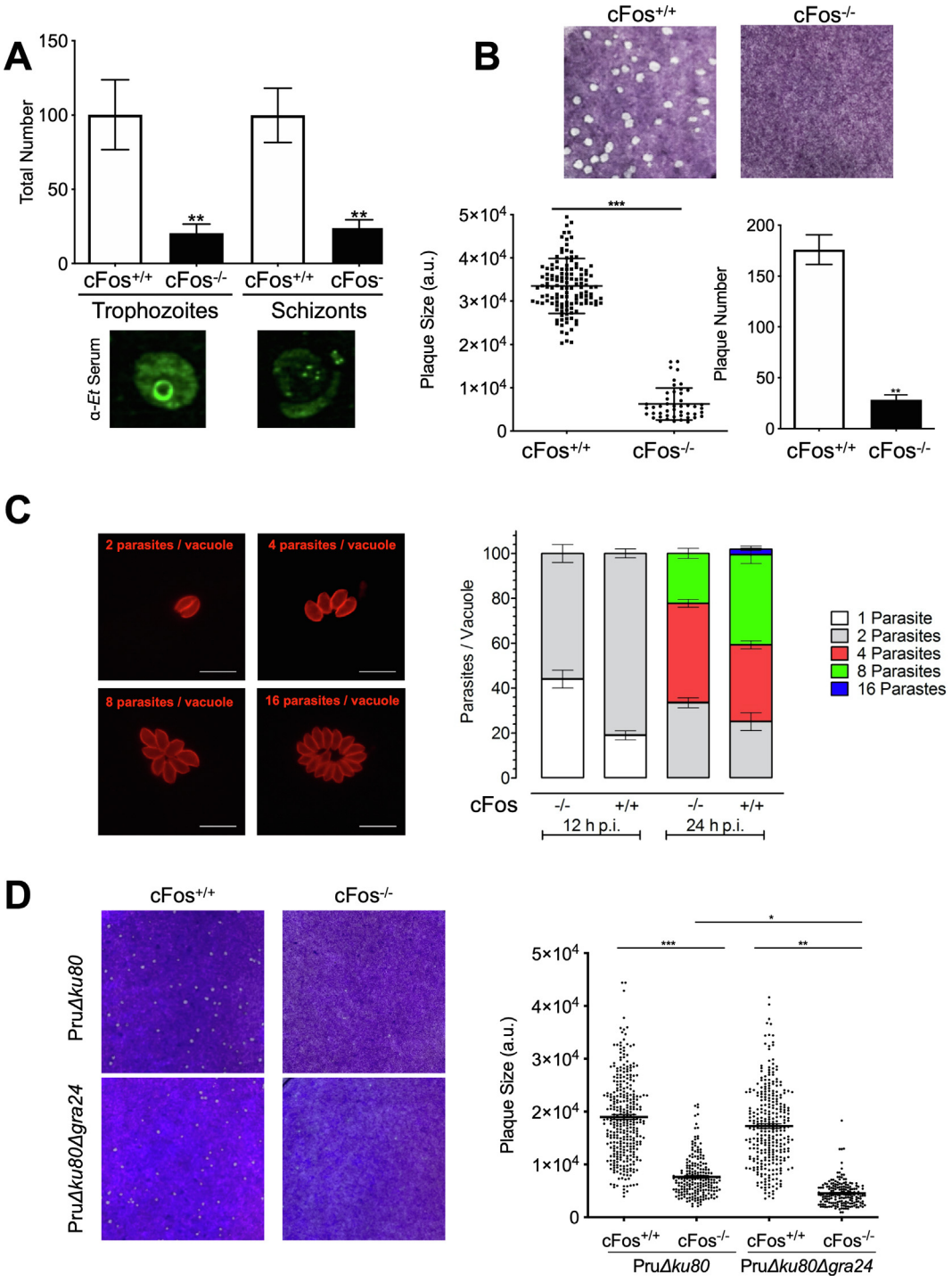

Fig. 4. Lack of cFos compromises the asexual growth of coccidian parasites in mouse fibroblasts. (A) Intracellular development of *E. falciformis* in MEF cells with or without cFos expression. The wild-type (cFos$^{+/+}$) or mutant (cFos$^{-/-}$) cells were infected with freshly isolated sporozoites of *E. falciformis*, and the developmental stages were quantified by immunostaining with cross-reactive anti-*E. tenella* serum. (B) Plaque assays representing the overall growth fitness of *T. gondii* tachyzoites in cFos$^{+/+}$ and cFos$^{-/-}$ cells. The white spots are formed by sequential lytic cycles of tachyzoites in a confluent monolayer of MEF cells (stained with crystal violet). (C) Intracellular replication of tachyzoites in MEF cells, as deduced by staining with anti-*Tg*Gap45 antibody. The mean fraction of the parasitophorous vacuoles enclosing variable number of tachyzoites are depicted in a bar graph (n = 3 assays, >400 vacuoles). (D) Plaques formed by the Pru*Δku80* (parental) and Pru*Δku80Δgra24* strains of *T. gondii* in cFos$^{+/+}$ and cFos$^{-/-}$ host cells. *Left panel* displays crystal violet-stained plaques in MEF monolayers, whereas the *confetti plot* (*right panel*) reveals the area of at least 200 plaques in arbitrary units (*a.u.*), as quantified by ImageJ program (n = 3 experiments; mean ± S.E.M.; *, $p \leq 0.05$; **, $p \leq 0.01$; ***, $p \leq 0.001$). (For interpretation of the references to color in this figure legend, the reader is referred to the web version of this article.)

($cFos^{-/-}$ MEFs). As expected, infection of the parental ($cFos^{+/+}$) MEF cells with *Eimeria* sporozoites resulted in the formation of schizont and trophozoite stages (Fig. 4A). In contrast, the development of these two parasite stages in cFos-knockout cells was strikingly reduced to 25%. A lack of cFos expression did not impact the sporozoite invasion into mutant MEFs, which was akin to the parental host cells (20% infection). A similar phenotype was observed when we examined the growth fitness of *T. gondii* tachyzoites in plaque assays using $cFos^{+/+}$ and $cFos^{-/-}$ MEFs (Fig. 4B). The wild-type cells supported the recurring lytic cycles of tachyzoites and, as anticipated, eventually led to the formation of plaques by disruption of confluent monolayers. In contrast, we scored a prominent reduction by > 75% in the number and size of plaques formed in the $cFos^{-/-}$ host cells.

A defect in plaque formation may be caused by impaired host-cell invasion, intracellular proliferation and/or egress of tachyzoites. Hence, we preformed additional phenotyping assays to determine the effect of cFos expression on individual steps of the lytic cycle. Both cell lines were parasitized equally (50%); however, the parasite replication was markedly reduced, as judged by counting tachyzoites within parasitophorous vacuoles during the course of infection (Fig. 4C). The fraction of large vacuoles (8–16 parasites/vacuole) was higher in the parental cells compared to cFos-knockout cells. Conversely, the latter host cells harbored a higher portion of smaller vacuoles (2–4 parasites/vacuole). The phenotype was evident even after 12 h infection, signifying that reproduction of tachyzoites in $cFos^{-/-}$ MEFs was arrested at an early stage. All above results taken together demonstrate a need of host cFos for the intracellular development of *Toxoplasma* tachyzoites and *Eimeria* sporozoites in mouse fibroblasts.

It has been previously reported that cFos can also be induced *via* an effector protein Gra24, secreted by a cyst-forming (type II) strain of *T. gondii* [25]. We therefore examined the growth fitness of parasites lacking the Gra24 expression (Fig. 4D). As expected, the parental strain (Pru*Δku80*) displayed a significantly impaired development in the $cFos^{-/-}$ host cells. A severe growth defect was also quite evident in the *Δgra24* mutant, suggesting that Gra24 does not underlie the specified phenotype in the cFos-knockout cells. Interestingly, we observed that when compared to the *Δgra24* mutant, the parental strain reproduced slightly better in the $cFos^{-/-}$ but not in the $cFos^{+/+}$ MEFs, which reflects a plausible role of Gra24 in promoting the parasite development in the absence of cFos expression.

2.5. Transcriptomics of parasitized $cFos^{+/+}$ and $cFos^{-/-}$ cells reveals a perturbation of cFos network

To decrypt how cFos can foster the coccidian development, we performed gene expression analysis of the wild-type ($cFos^{+/+}$) and cFos-knockout ($cFos^{-/-}$) MEFs infected with *Eimeria* or *Toxoplasma*, as shown for YAMC epithelial cells (Fig. 1). Infection-induced changes correlated between the parental and mutant MEFs for a large majority of genes notwithstanding the pathogen or infection period (Fig. 5A, see *Supplement Text*). There were nonetheless clear differences between the two host-cell types when infected by a given parasite. A small number (16 genes during *E. falciformis* and 20 during *T. gondii* infection) were inversely correlated, suggesting a divergent response of $cFos^{+/+}$ and $cFos^{-/-}$ cells (green dots, Fig. 5A). In both infections, we witnessed numerous transcripts that were uniquely induced or repressed either in the parental or cFos-knockout cells (Fig. 5B). In case of *Eimeria*, the number of altered genes was similar between the two cell types and time periods. *Toxoplasma*-infected $cFos^{-/-}$ cells by contrast displayed 2–4-fold fewer differentially-expressed genes in early and late cultures when compared to the $cFos^{+/+}$ host cells. The Venn diagram also showed a considerable number of commonly-regulated genes in the parental and mutant fibroblasts infected by individual parasites at a specified time point. These findings were further endorsed by Pearson correlation matrix (Fig S2A, refer to *Supplement Text* for additional details).

Of various plausible means to analyze our results, we first selected transcripts that were shared by YAMC and parental MEF cells upon infection with each parasite (Fig. 6A). We then filtered the chosen transcripts on the condition that they failed to be significantly modulated in cFos-knockout cells. Our approach eventually enriched only those genes that are likely to be cFos-dependent (cFos-related) and associated with infection. Our study yielded 384 and 187 genes differentially regulated by *T. gondii* and *E. falciformis*, respectively, in YAMC and $cFos^{+/+}$ but not in $cFos^{-/-}$ host cells. The GO-term analysis of these transcripts identified a repertoire of nucleotide-binding and ion-binding factors (Fig. 6A, Table S2). Intriguingly, while the former category dominated during *T. gondii* infection, the latter was more prominent in *Eimeria*-infected cells. A total of 18 genes were altered by both parasites in YAMC and wild-type MEF cells, which indicated a substantially minimal convergence between them.

We next validated the expression profile of 12 randomly-selected genes (Adar, Ccl4, Cldn1, Hes1, Peg10, Plxna4, Saa4, Sp100, Psmb8, Vcam1, Strbp, Zfp60) that were altered in both parental lines (YAMC and $cFos^{+/+}$ host cells), but unchanged in $cFos^{-/-}$ MEFs upon infection by tachyzoites of *T. gondii* (16 h) (Fig. 6B). As seen in microarray analysis, a majority of chosen transcripts (11 out of 12, except Ccl4) exhibited no significant modulation in $cFos^{-/-}$ MEFs. Besides, 7 genes (Adar, Ccl4, Cldn1, Hes1, Peg10, Plxna4, Saa4) displayed the same trend of regulation in both parental lines, as recorded by microarrays. Only 1 transcript (Vcam1) was differently modulated in the two wild-type host cells when compared to corresponding microarray data, and 4 genes (Sp100, Psmb8, Strbp, Zfp60) were inversely correlated either in YAMC epithelial or $cFos^{+/+}$ cells. In brief, the qPCR results added further confidence to our designated list of infection-relevant cFos-related genes.

2.6. cFos network associated with coccidian infection

In continuation of the above work, we constructed a cFos-centered protein–protein interaction network by STRING software (Fig. 6C). Indeed, 16 genes were directly networked with cFos and an additional panel of 39 genes were indirectly associated with cFos through its *primary* interaction network, which retrospectively endorsed our intersection analysis. Only 2 genes, Serpind1 and Ccl4, in the network were influenced by both parasites, whereas 16 others were either affected by *Eimeria* or *Toxoplasma*. The KEGG pathway classification of all genes appearing in the cFos-network enriched Ca^{2+}, MAPK and pattern recognition receptor signaling (Fig. 7). Not least, a direct comparison of KEGG pathways enriched among all infected host-cell types used herein disclosed an exclusive enrichment of insulin signaling in $cFos^{-/-}$ cells (Fig S3, Table S3). In conclusion, our comparative transcriptomics yielded an infection-relevant network of cFos comprising several deferentially-regulated putative determinants of coccidian development.

3. Discussion

Our transcriptomic analysis of the young adult mouse colonic epithelial cells infected with *Eimeria falciformis* or *Toxoplasma gondii* identified a large retinue of pathways, some of which were modulated by both, whereas others were regulated primarily by each pathogen. Infection-mediated reprogramming of YAMC epithelial cells signifies either host-cell defense and/or apparent

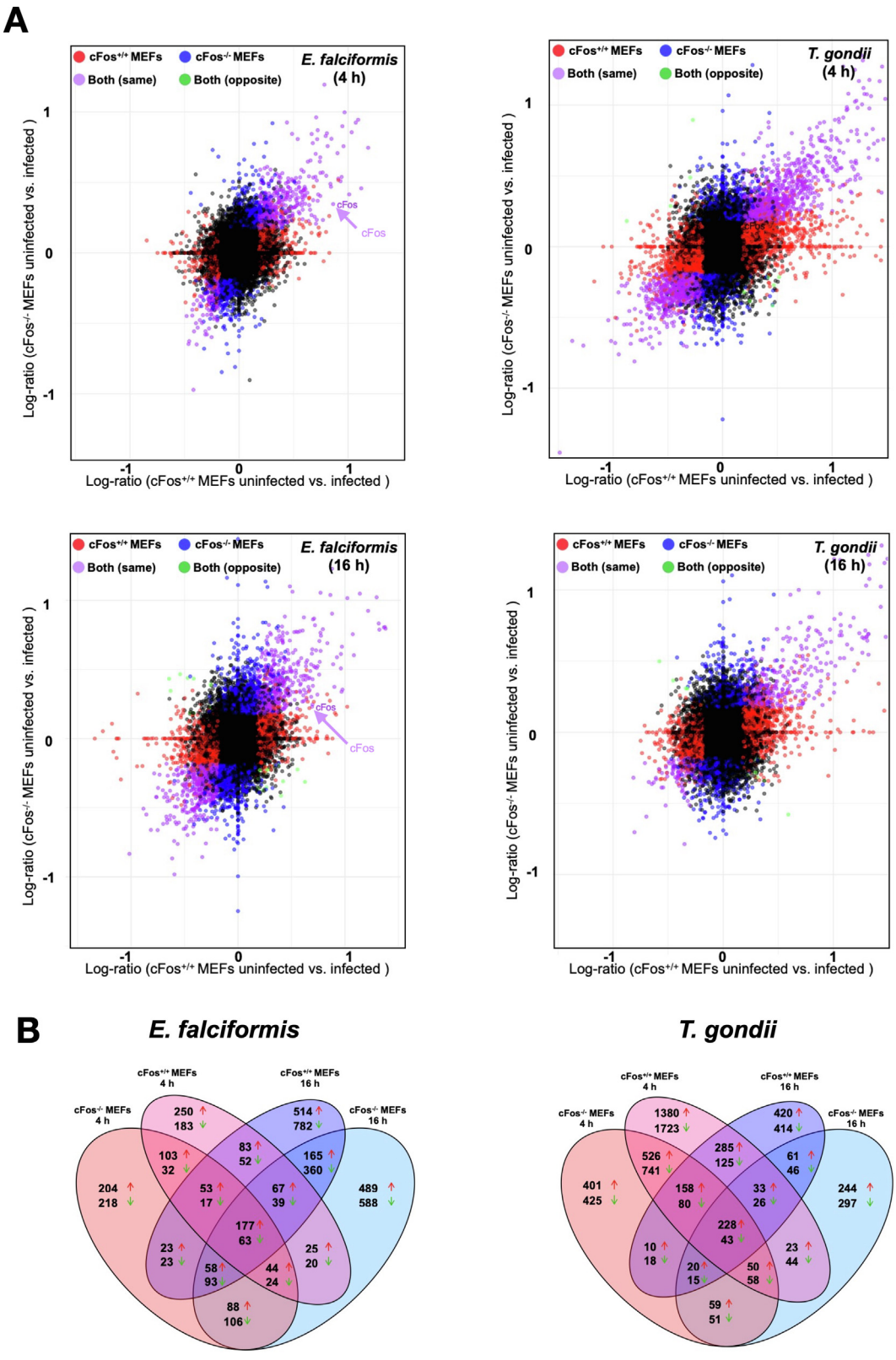

Fig. 5. Transcriptomic analysis of the wild-type and cFos-knockout mouse embryonic fibroblasts infected with *T. gondii* or *E. falciformis*. (A) Scatter plot illustrating the gene expression (fold-change) of cFos$^{+/+}$ and cFos$^{-/-}$ cells upon infection, as indicated. Differentially-regulated probes ($\geq$or $\leq$ 1.5, $p \leq 0.05$) are color-coded, whereas others appear in black. Transcripts altered only by *T. gondii* or by *E. falciformis* are presented in blue and red, respectively, while those regulated by both parasites are depicted in violet (same trend) or green (opposite trend). To see the complete correlation matrix (heatmap) of parasitized MEF and YAMC cells, refer to Fig. S2A. (B) Venn diagram of genes regulated upon infection by *T. gondii* or *E. falciformis*. (For interpretation of the references to color in this figure legend, the reader is referred to the web version of this article.)

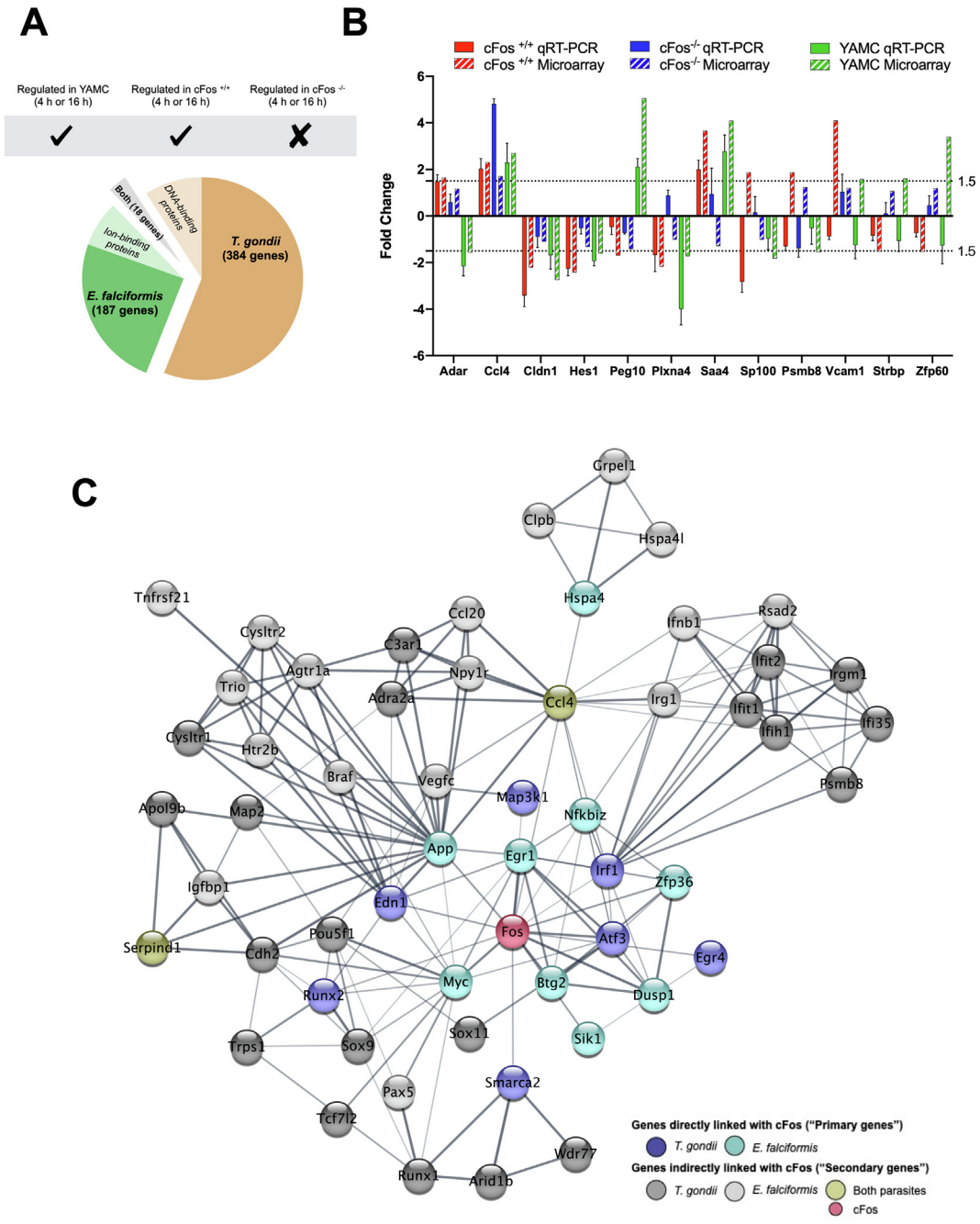

Fig. 6. Infection-relevant cFos-network as deduced by comparative transcriptomics of YAMC and MEF cells parasitized with *T. gondii* or *E. falciformis*. (A) Genes regulated in infected YAMC epithelial cells and in the parental MEFs but not in cFos$^{-/-}$ cells. The gene-ontology (GO) clusters most enriched upon *T. gondii* and *E. falciformis* infection are labeled. For other significant categories, refer to Table S2. The GO terms were enriched using DAVID v6.7 (threshold of EASE score ≤ 0.1). (B) Quantitative PCR illustrating the expression profile of 12 genes randomly selected from *panel A*. The bar graph shows a comparison of fold-change results, as calculated by the qPCR method and microarray analysis. Values $\geq$ or ≤ 1.5 were defined as 'significant' (dotted lines). (C) cFos-centered network predicted by STRING analysis of genes identified in *panel A*. The image shows *primary* genes (directly linked to cFos), and *secondary* genes (connected to cFos-networked *primary* genes). The breadth/thickness of connecting lines indicates the level of confidence. The *primary* genes were networked with STRING v11.0 at medium confidence (score ≥ 0.4), whereas the *secondary* genes were defined at high confidence (score ≥ 0.7).

subversion by the two parasites. A major group of differentially-expressed genes may, at least in part, be influenced by parasite-secreted proteins, as elaborated below. We found cFos as one of the 13 genes that were upregulated throughout the course of coccidian infection. Importantly, a lack of cFos expression retarded the growth of both parasites in murine embryonic fibroblast cells, advocating a pro-coccidian role of this transcription factor. In additional work using parasitized MEF and YAMC host cells, we discovered a cortege of cFos-networked factors related to infection irrespective of the host-cell type. Strikingly, genes differentially regulated in infected cells expressing cFos networked together and even cFos-related host signaling pathways were often shared, all of which plausibly act in consort to benefit *T. gondii* and *E. falciformis* (Fig. 7).

cFos belongs to an immediate early gene family of transcription factors, which is barely expressed under normal conditions but

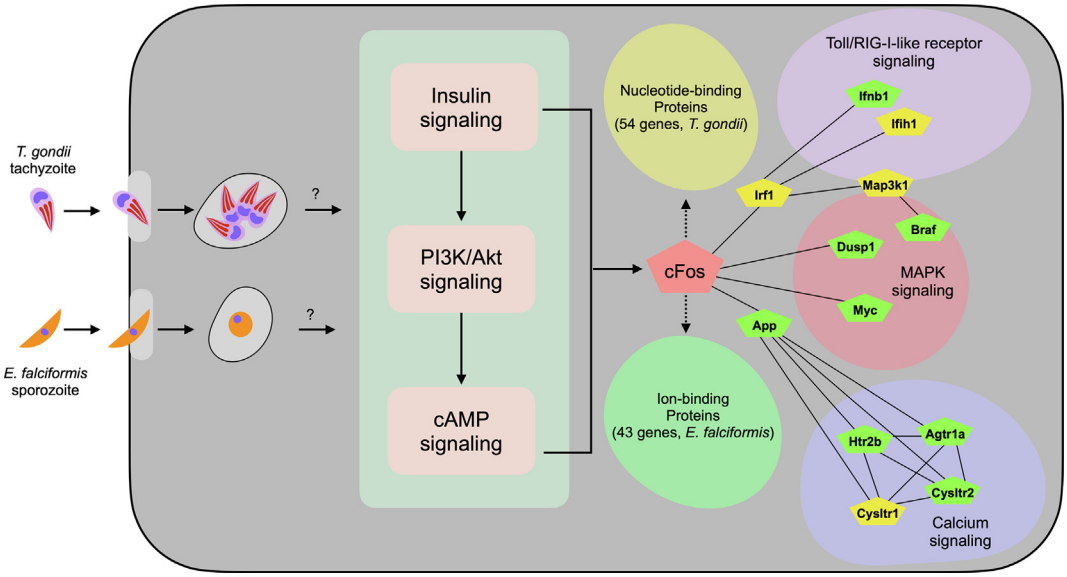

Fig. 7. A cFos-centered network of host proteins linked to intracellular parasitism by coccidians. The model was constructed based on the comparative gene expression analyses of YAMC and MEF ($cFos^{+/+}$ and $cFos^{-/-}$) cells infected by *T. gondii* or *E. falciformis*. The cFos-linked pathways influenced by both pathogens in the wild-type host cells include calcium, MAPK and pattern recognition receptor (Toll-/RIG-I like) signaling cascades. Several other genes encoding for nucleotide-binding and ion-binding proteins were affected by individual parasites. Note that according to our model, insulin signaling is enriched only in MEF host cells lacking cFos expression (Fig S3, Table S3), likely due to feedback regulation. Insulin, PI3K-Akt and cAMP signaling – differentially regulated upon coccidian infection – probably operate upstream of cFos. Transcriptomic reprogramming of the host cell may, at least in part, be driven by secretory effector molecules of the two parasites (*question-marked*).

rapidly induced by a repertoire of internal and external stimuli [17], such as by growth factors [26,27], cytokines [28], calcium [29], cAMP [30], oxidants [31], antioxidants [32], LPS [33], IFN-γ [34], as well as by physical [35] and mechanical [36] stress. Once induced, cFos and its family members (FosB, Fra-1, Fra-2) heterodimerize with members of the Jun family (cJun, JunB, JunD) to exert their function as transcription factors [37]. Heterodimerization results in the formation of AP-1 complex, which binds in the regulatory regions of many genes [38] and thereby controls differentiation, proliferation, apoptosis and immune response in a wide range of cell types [17,18]. The AP-1 complex has also been reported to be modulated by other pathogens *e.g.*, *Leishmania* [39,40], *Salmonella typhimurium* [41], *Bacillus anthracis* [42], hepatitis C virus [43] and polyomavirus [44]. Its activity correlates with oncogenic transformation and propagation of viruses [43,45–47]. On the other hand, AP-1 is known to facilitate the protective immunity against *Salmonella* [41] and *Leishmania* [39,40], and a lack of cFos promotes the growth of *S. typhimurium* [41]. Our findings on *T. gondii* and *E. falciformis* reverberate with the viral but contrast the bacterial pathogens, and thus epitomize opposing roles of cFos during infection by different pathogenic organisms.

We identified several cFos-networked factors involved in calcium, MAPK and RLR/TLR signaling, some of which are potentially subverted by coccidians. In accord, multiple transcripts of nucleotide and ion-binding proteins were modulated in infected YAMC and parental MEF but not in the $cFos^{-/-}$ host cells, suggesting a substantial transcriptional reprogramming associated with cFos expression (Fig. 7). Apicomplexan parasites are known to secrete an entourage of effector proteins from highly specialized organelles namely rhoptries, micronemes and dense granules [48]. Proteins discharged by the latter organelle usually enable adaptive modification of parasite-specific niches [49,50]. Tachyzoites of *T. gondii*, for instance, excrete many dense granule proteins (Gra15/16/24/44, IST *etc.*) that are known to modulate IFN, JAK-STAT, p38α MAPK, NF-κB and p53 signaling in host cells [25,51–56]. In context of this work, *Tg*Gra24 is reported to trigger prolonged autophosphorylation and nuclear translocation of the p38α MAP kinase [25,51], which correlates with the induction of immediate early genes. Similarly, *Tg*Gra16 and *Tg*Gra44 have been shown to induce cMyc in infected cells [52,57], and *Tg*IST counteracts the IFNβ and IFNγ-mediated defenses by binding to STAT1 and STAT1/STAT2 heterodimers [54]. Based on these studies, we surmise a role of dense granule proteins in the observed transcriptomic rewiring of YAMC and MEF cells. The genome of *E. falciformis* also encodes a broad range of predicted secretory factors [12]; however, the counterparts of *Toxoplasma* effector proteins are yet to be characterized.

Toxoplasma and *Eimeria* infection induced primarily discrete transcriptional response in a given host cell despite their close phylogenetic relationship. Similarly, different host cells of a selected organism displayed broadly distinct expression profile upon infection by individual parasites. Our comparative analysis disclosed regulation of multiple pathways in parasite- and/or host-specific manner (*Supplement Text*), some of which may underlie *in vitro* development of *E. falciformis*. Going further, a comparison of YAMC (*this work*) and caecum epithelial cells infected by *Eimeria* (*in vivo*) [8] might reveal additional determinants of parasite development. For example, tryptophan catabolism was one of the most outstanding (IFNγ-dependent) pathways by *ex vivo* transcriptomics, which we found to have a pro-parasite role *in vivo*. Even though numerous IFNγ-linked genes were regulated during *in vitro* infection of YAMC and MEF cells, tryptophan catabolism was not enriched in any of our datasets (Tables S4–S6). Similar observations were made with many IFNγ-regulated immunity-related GTPases and guanylate-binding proteins. *In vitro* optimization guided by comparative expression analyses therefore holds promise to develop a sustained culture of *E. falciformis*.

In conclusion, we demonstrate a physiological requirement of the mammalian cFos for intracellular development of *T. gondii* and *E. falciformis*. Additionally, we revealed an infection-affiliated network of cFos and signal cascades that are likely co-opted by coccidian parasites. A string of credible host determinants identified herein shall enable comprehensive dissection of pathogen-host interactions.

4. Materials and methods

4.1. Biochemical resources and bioethics statement

Oocysts of *Eimeria falciformis* were procured from Bayer (Germany), and tachyzoites of *Toxoplasma gondii* (type I RH strain) were provided by Carsten Lüder (Georg-August University, Germany). The cyst-forming type II strains of *T. gondii* (PruΔ*ku80*, Pru$\Delta\varpi$ *ku*80Δ*gra24*) were acquired from Mohamed Ali-Hakimi (University of Grenoble, France). The young adult mouse colonic epithelial cells were obtained from Robert Whitehead (Vanderbilt University, USA) [58]. The murine embryonic fibroblasts (parental, cFos$^{+/+}$ 1–98 M; mutant, cFos$^{-/-}$ 7–98 M) were offered by Marcus Christmann (University of Mainz, Germany) [59]. The primary antibodies recognizing *Tg*Sag1 (mouse) and *Tg*Gap45 (rabbit), and anti-*Eimeria tenella* serum (rabbit) were donated by Jean-François Dubremetz (University of Montpellier, France), Dominique Soldati-Favre (University of Geneva, Switzerland) and Fiona Tomley (Royal Veterinary College, London, UK), respectively. The primary antibody against the cFos protein (sc-271243) was purchased from Santa Cruz Biotechnology. NMRI mice were acquired from Charles River Laboratories (Sulzfeld, Germany). All animal experiments were executed following the guidelines of *Landesamt für Gesundheit und Soziales* (LaGeSo), Berlin.

4.2. Propagation of E. falciformis and sporozoite purification

The natural life cycle of *E. falciformis* was maintained by continuous passage in NMRI mice. In brief, oocysts were purified from animal feces by NaOCl floatation method [60], counted using a McMaster chamber, and stored in potassium dichromate at 4 °C for up to a maximum of 3 month. To isolate the free sporozoites, purified oocysts were digested with 0.4% pepsin (pH 3, 37 °C, 1 h), washed with PBS (1800*g*, 10 min), mixed with glass beads (0.5 mm, 1:1 ratio) and then vortexed briefly to release the sporocysts. Sporozoites were excysted by incubating the sporocyst preparation with 0.25% trypsin and 0.04% sodium tauroglycocholate (MP Biomedicals) in Dulbecco's modified Eagle's medium (DMEM) containing 2 mM glutamine, 100 μg/mL streptomycin and 100 U/mL penicillin (37 °C, 2 h), and then purified using DE52 anion-exchange chromatography, as described elsewhere [61].

4.3. The parasite and host cell culture

Tachyzoites of *T. gondii* were maintained in confluent monolayers of human foreskin fibroblast (HFF) cells, as reported previously [62]. HFFs were cultured in DMEM with 4.5 g/L glucose, 10% FCS, 2 mM glutamine, 1x MEM non-essential amino acids, 100 μg/mL streptomycin and 100 U/mL penicillin in a humidified incubator (37 °C, 5% CO_2). The YAMC epithelial cells were cultured in RPMI medium containing glucose (4.5 g/L), FCS (5%), insulin (1 μg/mL), α-thioglycerol (10 μM), hydrocortisone (1 μM) and IFNγ (5 U/mL) (33 °C, 5% CO_2). These cells originate from mice harboring a temperature-sensitive mutation of the SV40 large tumor antigen expressed under the control of a IFN-γ regulated MHCII promoter [58]. Hence, they require IFNγ and permissive temperature of 33 °C for optimal growth. The murine embryonic fibroblasts (cFos$^{+/+}$ 1–98 M wild-type and cFos$^{-/-}$ 7–98 M mutant) were cultured in DMEM supplemented with 4.5 g/L glucose, 10% FCS, 2 mM glutamine, 100 μg/mL streptomycin and 100 U/mL penicillin (37 °C, 5% CO_2). Host cells were harvested weekly by trypsinization method for routine propagation and seeded for infection, as indicated elsewhere. To perform the microarray analyses, we infected YAMC epithelial or MEF (wild-type and cFos-knockout) cells with tachyzoites of *T. gondii* (MOI: 2) or sporozoites of *E. falciformis* (MOI: 6), resulting in a normalized infection rate of about 40% across the host-cell types. We were not able to separate uninfected and infected cells; therefore, an impact of bystander cells on our final gene expression datasets cannot be excluded.

4.4. RNA isolation and microarray hybridization

Total RNA was isolated from uninfected and infected cells suspended in TRIzol (PureLink RNA kit, Life Technologies)[8], and analyzed for gene expression by dual-color hybridization using the whole-genome mouse microarray chips (4x44K, AMADID 014868, Agilent Technologies, Germany). We performed two biologically independent assays, each with dye-swapped replicates, and all sample-processing steps were executed according to the manufacturers' protocol. Briefly, 5 μg of purified RNA was reverse-transcribed, amplified and labeled with Cyanine 3-CTP or Cyanine 5-CTP using oligo-dT-T7 promoter primer (QuickAmp kit, Agilent Technologies). After precipitation, purification, quality test and quantification, 1 μg of each cRNA preparation was fragmented and hybridized overnight to microarrays, followed by washing steps, as recommended. Images were recorded using a laser scanner (G2565CA) at 5-μm resolution.

4.5. Computational analysis of microarray data

The microarray data were analyzed with the Agilent image analysis and feature extraction software using default settings (G2567AA). Dye ratios were calculated using the most conservative estimate between the universal and propagated error. The extracted MAGE-ML files were evaluated with the Rosetta Resolver Biosoftware. Only anti-correlated genes of dye-reversal hybridizations with $\geq$1.5-fold and an error-weighted *p*-value $\leq$0.05 were considered as differentially regulated. Microarray data have been deposited in the Gene Expression Omnibus (GEO; https://www.ncbi.nlm.nih.gov/geo), and can be accessed with the GEO accession number (GSE157395). Heatmaps were visualized with the R package "pheatmap" and/or GraphPad Prism (v8.0). The gene enrichment analysis was performed using the Database for Annotation, Visualization and Integrated Discovery (DAVID, v6.7) [63,64] (threshold of EASE score $\leq$0.1) and Kyoto Encyclopedia of Genes and Genomes (KEGG). cFos-centered network was predicted using the STRING program (v11.0) [65]. The *primary* genes directly networked with cFos were selected with a confidence score $\geq$0.4, while the *secondary* genes that were indirectly linked to cFos but directly networked with the *primary* genes were chosen with a confidence score $\geq$0.7.

4.6. Quantitative real-time PCR analysis

The YAMC epithelial cells infected with tachyzoites of the RH strain (MOI: 2; 16 h) were scraped in TRIzol solution for isolating the total RNA, which was immediately subjected to the cDNA synthesis using SuperScript III kit (Thermo Fisher Scientific). 10 ng cDNA of each sample was examined for the expression of designated transcripts by Platinum SYBR kit (20 μL reaction, Thermo Fisher Scientific). Samples from three independent assays were processed in duplicate reactions (Applied Biosystems 7300). The fold-change calculation was performed by the $^{\Delta\Delta}Ct$ method [66] using *rps18* as a housekeeping gene with respect to corresponding uninfected control groups. Primers for qPCR analysis of cFos family proteins were designed as reported elsewhere [67] (see Table S7 for all primers).

4.7. Indirect immunofluorescence assay

The parasitized host cell monolayers grown on coverslips were fixed with 4% paraformaldehyde (10 min), followed by neutralization with 0.1 M glycine/PBS (5 min, RT) and permeabilization by 0.2% Triton X-100/PBS (20 min). Samples were treated with 2% BSA in 0.2% Triton X-100/PBS (20 min) to minimize any unspecific binding of antibodies, and then incubated for 1 h with the primary antibody (anti-*Tg*Gap45, 1:10000; anti-cFos, 1:200) or anti-*Eimeria tenella* serum (1:2000, cross-reactive to *E. falciformis*). Samples were washed 3x with 0.2% Triton-X100/PBS (5 min), followed by addition of secondary antibodies (Alexa Fluor488 or 594, 1:3000, 45 min). After 3x washing steps with PBS, samples were mounted in Fluoromount G/DAPI and kept in dark at 4 °C. Imaging was performed by a fluorescence microscope (AxioVision, Zeiss, Germany).

4.8. The parasite phenotyping

All assays with tachyzoites of *T. gondii* were set up essentially as reported previously [68]. Parasitized HFF cells (MOI: 2–3; 36–44 h infection) were washed with the culture medium, scraped, and extruded through a 27G syringe (2x) to collect fresh extracellular parasites. For the invasion assay, host cells seeded on glass coverslips were infected with tachyzoites for 1 h (MOI: 6). Cells were subsequently fixed (4% paraformaldehyde, 15 min), neutralized (0.1 M glycine/PBS, 5 min) and then blocked (3% BSA/PBS, 30 min). Uninvaded or extracellular parasites were stained with anti-*Tg*Sag1 antibody (1:10000, 1 h) prior to detergent permeabilization. Cultures were washed 3x with PBS (5 min), permeabilized with 0.2% Triton-X 100/PBS (20 min), and then treated with anti-*Tg*Gap45 antibody (1:10000, 1 h) to detect invaded or intracellular parasites. Samples were finally washed and incubated with Alexa488 and Alexa594-conjugated secondary antibodies (1:3000, 1 h). Invasion efficiency was determined by counting parasites stained with anti-*Tg*Gap45/Alexa594 (in), but not with anti-*Tg*Sag1/Alexa488 (out). Invasion by *E. falciformis* sporozoites (MOI: 6) was assessed 4 h post-infection by counting the host cells per high power field (10 HPFs/sample, 400x magnification) after staining with cross-reactive anti-*E. tenella* serum, as mentioned above.

To set up the replication assay, host cells grown on coverslips were infected with $3x10^4$ tachyzoites (12–24 h infection) before fixation, permeabilization, neutralization, blocking and immunostaining with anti-*Tg*Gap45 and Alexa594 antibodies, as explained elsewhere. The cell division was assessed by enumerating intracellular parasites within their parasitophorous vacuoles. For the plaque assay, we cultured MEF cells to near-confluence in 6-well plates in standard culture medium, and then infected with 150–200 tachyzoites. The culture medium was adjusted to 1% FCS prior to infection to inhibit the overgrowth of uninfected cells, and cultures were kept at 37 °C for 7 days (12 days for Type II strain) without any perturbation. Samples were fixed with ice-cold methanol (-80 °C, 10 min), stained with crystal violet (12.5 g dye in 125 mL ethanol mixed with 500 mL of 1% ammonium oxalate) for 20 min and then washed with PBS to visualize plaques. The plaque size and number were measured by ImageJ program (National Institute of Health, USA).

Declaration of Competing Interest

The authors declare that they have no known competing financial interests or personal relationships that could have appeared to influence the work reported in this paper.

Acknowledgements

We thank Grit Meusel (Humboldt University, Berlin) for technical assistance, Enming Zhang (Castlepoint Systems, Australia) for initial support to process the microarray data, and the parasitology community for providing selected resources (parasite strains, host cells, antibodies etc.) as indicated elsewhere in this work. This study was funded by a standard research grant (GU1100/7) and Heisenberg program award (GU1100/16), endowed to NG by German Research Foundation (DFG). The funding agencies had no role in the design, execution, analyses, interpretation of the results, or decision to publish this work. We also acknowledge the Open Access Publication Fund of Humboldt University, Berlin.

Appendix A. Supplementary data

Supplementary data to this article can be found online at https://doi.org/10.1016/j.csbj.2020.12.045.

References

[1] Adl SM et al. Diversity, nomenclature, and taxonomy of protists. Syst Biol 2007;56:684–9.
[2] Ren B, Gupta N. Taming parasites by tailoring them. Front Cell Infect Microbiol 2017;7:292.
[3] Braun L et al. The Toxoplasma effector TEEGR promotes parasite persistence by modulating NF-kappaB signalling via EZH2. Nat Microbiol 2019;4:1208–20.
[4] Gay G et al. Toxoplasma gondii TgIST co-opts host chromatin repressors dampening STAT1-dependent gene regulation and IFN-gamma-mediated host defenses. J Exp Med 2016;213:1779–98.
[5] He H et al. Characterization of a Toxoplasma effector uncovers an alternative GSK3/beta-catenin-regulatory pathway of inflammation. Elife 2018;7.
[6] Duszynski DW. Eimeria. Wiley; 2011.
[7] Schmid M, Lehmann MJ, Lucius R, Gupta N. Apicomplexan parasite, *Eimeria falciformis*, co-opts host tryptophan catabolism for life cycle progression in mouse. J Biol Chem 2012;287(24):20197–207.
[8] Schmid M et al. *Eimeria falciformis* infection of the mouse caecum identifies opposing roles of IFNgamma-regulated host pathways for the parasite development. Mucosal Immunol 2014;7:969–82.
[9] Ehret T, Spork S, Dieterich C, Lucius R, Heitlinger E. Dual RNA-seq reveals no plastic transcriptional response of the coccidian parasite *Eimeria falciformis* to host immune defenses. BMC Genomics 2017;18:686.
[10] Huang G et al. Influence of *Eimeria falciformis* infection on gut microbiota and metabolic pathways in mice. Infect Immun 2018;86.
[11] Jarquín-Díaz VH et al. Detection and quantification of house mouse Eimeria at the species level – challenges and solutions for the assessment of coccidia in wildlife. Int J Parasitol: Parasites and Wildlife 2019;10:29–40.
[12] Heitlinger E, Spork S, Lucius R, Dieterich C. The genome of *Eimeria falciformis*–reduction and specialization in a single host apicomplexan parasite. BMC Genomics 2014;15:696.
[13] Balard A et al. Intensity of infection with intracellular Eimeria spp. and pinworms is reduced in hybrid mice compared to parental subspecies. J Evol Biol 2020;33(4):435–48.
[14] Jarquín-Díaz VH et al. Generalist Eimeria species in rodents: multilocus analyses indicate inadequate resolution of established markers. Ecol Evol 2020;10(3):1378–89.
[15] Kong P, Lehmann MJ, Helms JB, Brouwers JF, Gupta N. Lipid analysis of Eimeria sporozoites reveals exclusive phospholipids, a phylogenetic mosaic of endogenous synthesis, and a host-independent lifestyle. Cell Discov 2018;4:24.
[16] Pogonka T et al. CD8+ cells protect mice against reinfection with the intestinal parasite *Eimeria falciformis*. Microbes Infect 2010;12(3):218–26.
[17] Hess J, Angel P, Schorpp-Kistner M. AP-1 subunits: quarrel and harmony among siblings. J Cell Sci 2004;117:5965–73.
[18] Durchdewald M, Angel P, Hess J. The transcription factor Fos: a Janus-type regulator in health and disease. Histol Histopathol 2009;24:1451–61.
[19] Smith JE. A ubiquitous intracellular parasite: the cellular biology of Toxoplasma gondii. Int J Parasitol 1995;25(11):1301–9.
[20] Kovacs KJ. c-Fos as a transcription factor: a stressful (re)view from a functional map. Neurochem Int 1998;33:287–97.
[21] Zinatizadeh MR, Momeni SA, Zarandi PK, Chalbatani GM, Dana H, Mirzaei HR, Akbari ME, Miri SR. The role and function of Ras-association domain family in cancer: a review. Genes & Diseases 2019;6(4):378–84.
[22] Agac D, Estrada LD, Maples R, Hooper LV, Farrar JD. The beta2-adrenergic receptor controls inflammation by driving rapid IL-10 secretion. Brain Behav Immun 2018;74:176–85.
[23] Park S-M et al. IKZF2 drives leukemia stem cell self-renewal and inhibits myeloid differentiation 153-165 e157. Cell Stem Cell 2019;24(1).
[24] Derebe MG et al. Serum amyloid A is a retinol binding protein that transports retinol during bacterial infection. Elife 2014;3. e03206.
[25] Braun L et al. A Toxoplasma dense granule protein, GRA24, modulates the early immune response to infection by promoting a direct and sustained host p38 MAPK activation. J Exp Med 2013;210:2071–86.
[26] Hayes TE, Kitchen AM, Cochran BH. Inducible binding of a factor to the c-fos regulatory region. Proc Natl Acad Sci 1987;84(5):1272–6.

[27] Fu X-Y, Zhang J-J. Transcription factor p91 interacts with the epidermal growth factor receptor and mediates activation of the c-fos gene promoter. Cell 1993;74(6):1135–45.
[28] Shibuya H et al. Functional dissection of p56lck, a protein tyrosine kinase which mediates interleukin-2-induced activation of the c-fos gene.. Mol Cell Biol 1994;14(9):5812–9.
[29] Sheng M, McFadden G, Greenberg ME. Membrane depolarization and calcium induce c-fos transcription via phosphorylation of transcription factor CREB. Neuron 1990;4(4):571–82.
[30] Fisch TM, Prywes R, Simon MC, Roeder RG. Multiple sequence elements in the c-fos promoter mediate induction by cAMP.. Genes Dev 1989;3(2):198–211.
[31] Nose K et al. Transcriptional activation of early-response genes by hydrogen peroxide in a mouse osteoblastic cell line. Eur J Biochem 1991;201:99–106.
[32] Meyer M, Schreck R, Baeuerle PA. H2O2 and antioxidants have opposite effects on activation of NF-kappa B and AP-1 in intact cells: AP-1 as secondary antioxidant-responsive factor. EMBO J 1993;12(5):2005–15.
[33] Wan W, Wetmore L, Sorensen CM, Greenberg AH, Nance DM. Neural and biochemical mediators of endotoxin and stress-induced c-fos expression in the rat brain. Brain Res Bull 1994;34(1):7–14.
[34] Rubio N. Interferon-gamma induces the expression of immediate early genes c-fos and c-jun in astrocytes. Immunology 1997;91:560–4.
[35] Buscher M, Rahmsdorf HJ, Litfin M, Karin M, Herrlich P. Activation of the c-fos gene by UV and phorbol ester: different signal transduction pathways converge to the same enhancer element. Oncogene 1988;3:301–11.
[36] Grembowicz KP, Sprague D, McNeil PL, Guidotti G. Temporary disruption of the plasma membrane is required for c-fos expression in response to mechanical stress. MBoC 1999;10(4):1247–57.
[37] Chiu R et al. The c-Fos protein interacts with c-Jun/AP-1 to stimulate transcription of AP-1 responsive genes. Cell 1988;54:541–52.
[38] Angel P, Karin M. The role of Jun, Fos and the AP-1 complex in cell-proliferation and transformation. Biochim Biophys Acta (BBA) 1991;1072(2-3):129–57.
[39] Descoteaux A, Matlashewski G. c-fos and tumor necrosis factor gene expression in *Leishmania donovani*-infected macrophages.. Mol Cell Biol 1989;9(11):5223–7.
[40] Contreras I et al. Leishmania-induced inactivation of the macrophage transcription factor AP-1 is mediated by the parasite metalloprotease GP63. PLoS Pathogens 2010;6. e1001148.
[41] Maruyama K, Sano G-I, Ray N, Takada Y, Matsuo K. c-Fos-deficient mice are susceptible to salmonella enterica serovar typhimurium infection. Infect Immun 2007;75(3):1520–3.
[42] Comer JE et al. Murine macrophage transcriptional and functional responses to Bacillus anthracis edema toxin. Microb Pathog 2006;41(2-3):96–110.
[43] Kang SM et al. c-Fos regulates hepatitis C virus propagation. FEBS Letters 2011;585:3236–44.
[44] Glenn GM, Eckhart W. Transcriptional regulation of early-response genes during polyomavirus infection. J Virol 1990;64:2193–201.
[45] Tsutsumi T et al. Alteration of intrahepatic cytokine expression and AP-1 activation in transgenic mice expressing hepatitis C virus core protein. Virology 2002;304:415–24.
[46] Koike K. Pathogenesis of HCV-associated HCC: dual-pass carcinogenesis through activation of oxidative stress and intracellular signaling. Hepatol Res 2007;37(Suppl. 2):S115–20.
[47] Mahata S et al. Berberine modulates AP-1 activity to suppress HPV transcription and downstream signaling to induce growth arrest and apoptosis in cervical cancer cells. Mol Cancer 2011;10(1):39.
[48] Gubbels M-J, Duraisingh MT. Evolution of apicomplexan secretory organelles. Int J Parasitol 2012;42(12):1071–81.
[49] Rastogi S, Cygan AM, Boothroyd JC. Translocation of effector proteins into host cells by Toxoplasma gondii. Curr Opin Microbiol 2019;52:130–8.
[50] Hakimi M-A, Olias P, Sibley LD. Toxoplasma effectors targeting host signaling and transcription. Clin Microbiol Rev 2017;30(3):615–45.
[51] Mercer HL et al. *Toxoplasma gondii* dense granule protein GRA24 drives MyD88-independent p38 MAPK activation, IL-12 production and induction of protective immunity. PLoS Pathog 2020;16.
[52] Blakely WJ, Holmes MJ, Arrizabalaga G. The secreted acid phosphatase domain-containing GRA44 from Toxoplasma gondii is required for c-Myc induction in infected cells. mSphere 2020;5.
[53] Sangare LO et al. Toxoplasma GRA15 activates the NF-kappaB pathway through interactions with TNF receptor-associated factors. mBio 2019;10.
[54] Matta SK et al. Toxoplasma gondii effector TgIST blocks type I interferon signaling to promote infection. Proc Natl Acad Sci USA 2019;116 (35):17480–91.
[55] Kim S-G et al. Increase in the nuclear localization of PTEN by the Toxoplasma GRA16 protein and subsequent induction of p53-dependent apoptosis and anticancer effect. J Cell Mol Med 2019;23(5):3234–45.
[56] Bougdour A et al. Host cell subversion by toxoplasma GRA16, an exported dense granule protein that targets the host cell nucleus and alters gene expression. Cell Host Microbe 2013;13(4):489–500.
[57] Panas MW, Boothroyd JC. Toxoplasma uses GRA16 to upregulate host c-Myc. mSphere 2020;5.
[58] Whitehead RH, VanEeden PE, Noble MD, Ataliotis P, Jat PS. Establishment of conditionally immortalized epithelial cell lines from both colon and small intestine of adult H-2Kb-tsA58 transgenic mice:. Proc Natl Acad Sci 1993;90 (2):587–91.
[59] Lackinger D, Kaina B. Primary mouse fibroblasts deficient for c-Fos, p53 or for both proteins are hypersensitive to UV light and alkylating agent-induced chromosomal breakage and apoptosis. Mutat Res/Fundam Mol Mech Mutag 2000;457(1-2):113–23.
[60] Stockdale PG, Stockdale MJ, Rickard MD, Mitchell GF. Mouse strain variation and effects of oocyst dose in infection of mice with *Eimeria falciformis*, a coccidian parasite of the large intestine. Int J Parasitol 1985;15:447–52.
[61] Schmatz DM, Crane MS, Murray PK. Purification of Eimeria sporozoites by DE-52 anion exchange chromatography. J Protozool 1984;31:181–3.
[62] Gupta N, Zahn MM, Coppens I, Joiner KA, Voelker DR. Selective disruption of phosphatidylcholine metabolism of the intracellular parasite *Toxoplasma gondii* arrests its growth. J Biol Chem 2005;280(16):16345–53.
[63] Huang da W, Sherman BT, Lempicki RA. Bioinformatics enrichment tools: paths toward the comprehensive functional analysis of large gene lists. Nucl Acids Res 2009;37:1–13.
[64] Huang DW, Sherman BT, Lempicki RA. Systematic and integrative analysis of large gene lists using DAVID bioinformatics resources. Nat Protoc 2009;4 (1):44–57.
[65] Szklarczyk D et al. STRING v11: protein-protein association networks with increased coverage, supporting functional discovery in genome-wide experimental datasets. Nucl Acids Res 2019;47:D607–13.
[66] Livak KJ, Schmittgen TD. Analysis of relative gene expression data using real-time quantitative PCR and the 2(-Delta Delta C(T)) method. Methods 2001;25:402–8.
[67] Terao A, Greco MA, Davis RW, Heller HC, Kilduff TS. Region-specific changes in immediate early gene expression in response to sleep deprivation and recovery sleep in the mouse brain. Neuroscience 2003;120(4):1115–24.
[68] Arroyo-Olarte RD et al. Phosphatidylthreonine and lipid-mediated control of parasite virulence. PLoS Biol 2015;13. e1002288.